OPEN ACCESS

International
Journal
Of Modern Engineering Research (IJMER)

Micromechanical Modeling of the Macroscopic Behavior of Soft Ferromagnetic Composites

Ke Jin[1], Yong Kou[2], Jacob Aboudi*[3]

[1,2]*School Of Aerospace Science And Technology Xidian University Xi'an, Shanxi 710126, PR China*
[3]*School Of Mechanical Engineering Tel Aviv University Ramat Aviv 69978, Israel*

ABSTRACT: Soft ferromagnetic composites consist of ferromagnetic particles embedded within non-magnetic electrically insulating matrix. The aims of this article are twofold. In the first one, multiaxial nonlinear isothermal constitutive equations that govern the behavior of soft ferromagnetic materials are generalized to include the temperature and hysteretic effects. The second aim consists of developing a micromechanical analysis which takes into account the detailed interaction between the phases, and establishes the instantaneous concentration tensors which relate between the local magneto-thermo-elastic field and the externally applied loading. The ferromagnetic particles constituents employed in the micromechanical analysis are governed by the developed magneto-thermo-elastic coupled hysteretic constitutive relations. With the established concentration tensors, the macroscopic (global) re- sponse of the composite can be readily determined at any instant of loading. The offered micromechanical modeling is capable of predicting the response of soft ferromagnetic composites that are subjected to various types of magneto-thermo-elastic loadings, and it can be employed by the designer to easily determine the composite response for a particular desired application.

Keywords: *Magnetostriction, Soft Ferromagnetic Materials, Magnetostrictive compos- ites, Micromechanics analysis. High-fidelity generalized method of cells.*

I. INTRODUCTION

Soft ferromagnetic materials, such as medium-carbon steel, can be easily magnetized and demagnetized. The magnetostriction (the induced strains by applied magnetic field) of these materials is very small, of the order of 10^{-6}, as compared to giant magnetostrictive materials (e.g. Terfenol- D which is a metallic compound) which is of the order of 10^{-3}. The strain of the latter increases monotonically with the applied magnetic field (e.g. Moffet et al. (1991)), but the strain in medium-carbon steel increases first with the applied magnetic field, but then drops, Gorkunov et al. (2013). Furthermore, the constitutive equations of soft ferromagnetic materials are more complicated than those of giant magnetostrictive materials in the sense that the magnetoelastic coupling terms in the former require the inclusion of M2 and M4 (M is the magnetization), whereas in the latter only terms involving M2 are included, Zhou et al. (2009).

Soft ferromagnetic composites consist of soft ferromagnetic particles dispersed in a non- magnetic matrix which is usually taken as an electrically insulating polymer (e.g. epoxy resin). By using a polymer as a matrix, the resulting magnetic composite can be molded in various de- sired shape. This type of composite materials can be used in various applications such as electric motors, transformers and electromagnetic wave shielding, see Hultman and Jack (2003), Guo et al. (2003), Bayramli et al. (2005), Hamler et al. (2006), Svensson et al. (2012) and Ruffini et al. (2014), for example. Furthermore, since the magnetostriction of soft ferromagnetic composites is very small, they can be employed to reduce the noise levels caused by vibrations of electromag- netic machines. A review of soft magnetic composites is given by Shokrollahi and Janghorban (2007), where a literature review, applications and material selection are discussed.

The values of the volume fraction of the soft ferromagnetic material in the composites vary depending on the application. The polymer may be employed just for the coating of the particles, e.g., Shokrollahi and Janghorban (2007), or by adding small amount of the polymer to electrically insulate the particles, e.g., Streckova et al. (2013), Dias et al. (2013), Streckova et al. (2015), and in Gramatyka et al. (2006), for example, a 5 percent resin volume fraction has been reported. In some other investigations significant values of soft ferromagnetic material have been reported, see Svensson et al. (2012) where a 70 percent of particles have been reported. In Nowosielski (2007), the content of powder particles mass content varies from 50 to 90 percent, and from 3 50 to 96 volume percent have been reported by Tada and Suzuki (2002). In Bednarek (1997), experiments have been performed in which the ferromagnetic material volume fraction changed from 0.05 to

0.95.

Multiaxial nonlinear constitutive equations for soft ferromagnetic materials that do not in- clude thermal and hysteretic effects have been proposed by Zhou et al. (2009). In the present investigation, these constitutive relations are first generalized to include the coupled magneto- thermo-elastic hysteretic effects. Subsequently, these coupled multiaxial nonlinear constitutive relations are employed in a micromechanical model for the prediction of the macroscopic (global) behavior of soft ferromagnetic composites. To the authors knowledge, the only investigations which model the behavior of soft ferromagnetic composites are those who predict the effective permeability, see Bednarek (1997) and Paterson et al. (1999), for example.

In the present investigation, the high-fidelity generalized method of cells (HFGMC) nonlinear micromechanics analysis is employed to establish the overall response of the soft ferromagnetic composites. This micromechanical model has been employed to model composites of various types, and the veracity of its predictions have been illustrated in various circumstances, see Aboudi et al. (2013) which present and discuss the HFGMC in general, and its applications on smart composites in particular. The HFGMC has been recently employed for the prediction of the behavior of magnetostrictive composites, Aboudi et al. (2014). In the present investigation this micromechanics model is further applied to predict the behavior of soft ferromagnetic composites by employing the generalized coupled magneto-thermo-elastic of soft ferromagnetic materials with hysteretic effects. This modeling should allows the designer to easily determine the composite response (magnetostriction, magnetic flux density and effective permeability) for a particular desired application.

The present article is organized as follows. In Section 2, the generalized coupled constitutive relations, the governing equations and interfacial conditions are presented. In the following section a brief description of the nonlinear HFGMC model is given. This is followed by the applications section and conclusions.

II. CONSTITUTIVE AND GOVERNING EQUATIONS OF SOFT FERRO- MAGNETIC MATERIALS

The isothermal multiaxial nonlinear constitutive equations of soft ferromagnetic materials which do not include hysteretic effects have been offered by Zhou et al. (2009). In the present section, a generalization of these equations is given, resulting into multiaxial magneto-thermo-elastic coupled hysteretic constitutive relations.

Consider an isotropic ferromagnetic material that is subjected to an applied stress σij , i, j = 1, 2, 3, and a magnetic field intensity Hi at temperature θ. The elastic Gibbs energy, formulated in terms of the independent variables (σ_{ij} , M_i, S), is defined by, (Smith (2005), Zhou et al. (2009))

$$G(\sigma_{ij}, M_i, \theta) = U - \theta S - \sigma_{ij}\epsilon_{ij} \tag{1}$$

where ϵ_{ij}, M_i and S are the components of the strain, magnetization and the scalar entropy density, respectively. The change in the internal energy U is given by the total differential

$$dU = \sigma_{ij} d\epsilon_{ij} + \mu_0 H_i dM_i + \theta dS \tag{2}$$

where $\mu_0 = 4\pi \times 10^{-7}$ H/m is the vacuum permeability.

Consequently, the following thermodynamic relations can be derived:

$$\epsilon_{ij} = -\frac{\partial G}{\partial \sigma_{ij}}, \quad \mu_0 H_k = \frac{\partial G}{\partial M_k}, \quad S = -\frac{\partial G}{\partial \theta} \tag{3}$$

Expanding G at the point $(\sigma_{ij} = 0, M_i = 0, \theta_0)$, where θ_0 is the room temperature chosen as reference temperature, yields

$$G(\epsilon_{ij}, M_i, \theta) = G_0 + \frac{\partial G}{\partial \sigma_{ij}}\sigma_{ij} + \frac{\partial G}{\partial M_i}M_i + \frac{\partial G}{\partial \theta}(\theta - \theta_0) + \frac{1}{2}A^2 G + \frac{1}{3!}A^3 G + ... \tag{4}$$

where the operator A is defined as

$$A = \sigma_{ij}\frac{\partial}{\partial \sigma_{ij}} + M_i\frac{\partial}{\partial M_i} + (\theta - \theta_0)\frac{\partial}{\partial \theta}$$

The constant G_0, the linear terms and odd order terms of M_i in (4) can be neglected due to the symmetric properties about the magnetization variable, a detailed discussion see Zhou et al. (2009). As a result, the strain and magnetic field components can be written in the form

$$\begin{aligned}
\epsilon_{ij} &= -\frac{\partial^2 G}{\partial\sigma_{ij}\sigma_{mn}}\sigma_{mn} - \frac{1}{2}\frac{\partial^3 G}{\partial\sigma_{ij}\sigma_{mn}\sigma_{rs}}\sigma_{mn}\sigma_{rs} + \ldots - \frac{\partial^2 G}{\partial\sigma_{ij}\partial\theta}(\theta-\theta_0) + \ldots \\
&- \frac{1}{2}\left[\frac{\partial^3 G}{\partial\sigma_{ij}\partial M_k\partial M_l} + \frac{\partial^4 G}{\partial\sigma_{ij}\sigma_{mn}\partial M_k\partial M_l}\sigma_{mn} + \frac{\partial^4 G}{\partial\sigma_{ij}\partial M_k\partial M_l\partial\theta}(\theta-\theta_0) + \ldots\right] M_k M_l \\
&- \frac{1}{24}\left[\frac{\partial^5 G}{\partial\sigma_{ij}\partial M_k\partial M_l\partial M_p\partial M_q} - \frac{\partial^6 G}{\partial\sigma_{ij}\partial\sigma_{mn}\partial M_k\partial M_l\partial M_p\partial M_q}\sigma_{mn}\right. \\
&- \left.\frac{\partial^6 G}{\partial\sigma_{ij}\partial M_k\partial M_l\partial M_p\partial M_q\partial\theta}(\theta-\theta_0)\right] M_k M_l M_p M_q + \ldots \qquad (5)
\end{aligned}$$

$$\begin{aligned}
\mu_0 H_k &= \left[\frac{\partial^2 G}{\partial M_k\partial M_l} + \frac{\partial^3 G}{\partial M_k\partial M_l\partial\theta}(\theta-\theta_0)\right] M_l \\
&+ \frac{1}{6}\left[\frac{\partial^4 G}{\partial M_k\partial M_l\partial M_p\partial M_q} + \ldots + \frac{\partial^5 G}{\partial M_k\partial M_l\partial M_p\partial M_q\partial\theta}(\theta-\theta_0)\right] M_l M_p M_q + \ldots \\
&+ \left[\frac{\partial^3 G}{\partial\sigma_{ij}\partial M_k\partial M_l}\sigma_{ij} + \frac{1}{2}\frac{\partial^4 G}{\partial\sigma_{ij}\partial\sigma_{mn}\partial M_k\partial M_l}\sigma_{ij}\sigma_{mn}\right] M_l \\
&+ \frac{1}{6}\left[\frac{\partial^5 G}{\partial\sigma_{ij}\partial M_k\partial M_l\partial M_p\partial M_q}\sigma_{ij} + \frac{1}{2}\frac{\partial^6 G}{\partial\sigma_{ij}\partial\sigma_{mn}\partial M_k\partial M_l\partial M_p\partial M_q}\sigma_{ij}\sigma_{mn}\right] M_l M_p M_q + \ldots \\
&+ \frac{\partial^4 G}{\partial\sigma_{ij}\partial M_k\partial M_l\partial\theta}\sigma_{ij}M_l(\theta-\theta_0) + \frac{1}{6}\frac{\partial^6 G}{\partial\sigma_{ij}\partial M_k\partial M_l\partial M_p\partial M_q\partial\theta}\sigma_{ij}M_l M_p M_q(\theta-\theta_0) \qquad (6)
\end{aligned}$$

The expression for the strain components in Eq. (5) consists of four parts. The first part is the elastic strain produced by stress. Since stress would changes the orientations of magnetic domains in ferromagnetic material, the first part for isotropic material, reduces to, Jin et al. (2012),

$$-\frac{\partial^2 G}{\partial\sigma_{ij}\sigma_{mn}}\sigma_{mn} - \frac{1}{2}\frac{\partial^3 G}{\partial\sigma_{ij}\sigma_{mn}\sigma_{rs}}\sigma_{mn}\sigma_{rs} + \ldots = \frac{1}{E}\left[(1+\nu)\sigma_{ij} - \nu\sigma_{mm}\delta_{ij}\right] + \lambda_s\frac{\tilde{\sigma}_{ij}}{\sigma_s} \qquad (7)$$

where the intrinsic elasticity and the elastic strain dependent on the domain rotation are included, E and ν are the Young's modulus and Poisson's ratio, respectively, δ_{ij} is the Kronecker delta, λ_s is the maximum magnetostrictive strain and σ_s is a stress parameter. In addition, $\tilde{\sigma}_{ij} = 3\sigma_{ij}/2 - \sigma_{mm}\delta_{ij}/2$.

The second part in Eq. (5) represents the thermal expansion strain, which for isotropic material takes the form

$$-\frac{\partial^2 G}{\partial\sigma_{ij}\partial\theta}(\theta-\theta_0) = \bar{\alpha}(\theta-\theta_0)\delta_{ij} \qquad (8)$$

where $\bar{\alpha}$ is the coefficient of thermal expansion of the material. The third and fourth part in Eq. (5) includes magnetostrictive strain and the strain item concerning magneto-thermal coupling. Adopting the quadratic and quartic laws of the magne- tostriction of ferromagnetic materials, Jiles (1995), the third part (i.e., the expressions involvingM_kM_l) in Eq. (5) can be written as

$$\begin{aligned} & -\frac{1}{2}\left[\frac{\partial^3 G}{\partial\sigma_{ij}\partial M_k\partial M_l}+\frac{\partial^4 G}{\partial\sigma_{ij}\sigma_{mn}\partial M_k\partial M_l}\sigma_{mn}+\ldots+\frac{\partial^4 G}{\partial\sigma_{ij}\partial M_k\partial M_l\partial\theta}(\theta-\theta_0)+\ldots\right]M_kM_l \\ & =\frac{1}{M_{ws}^2}\left[\frac{3\lambda_s}{2}\delta_{ik}\delta_{jl}-\frac{\lambda_s}{2}\delta_{kl}\delta_{ij}-\frac{\lambda_s}{\sigma_s}\bar{\sigma}_{ij}\delta_{kl}+\bar{\beta}(\theta-\theta_0)\delta_{ij}\delta_{kl}\right]M_kM_l \\ & =\frac{1}{M_{ws}^2}\left\{\frac{3\lambda_s}{2}M_iM_j-M_kM_k\left[\frac{\lambda_s}{2}\delta_{ij}+\frac{\lambda_s}{\sigma_s}\bar{\sigma}_{ij}-\bar{\beta}(\theta-\theta_0)\delta_{ij}\right]\right\} \end{aligned} \tag{9}$$

where the parameter M_{ws} denotes the saturation magnetization when domain wall motions are completed, i.e. the saturation domain wall motion magnetization when the stress is zero , Zhou et al. (2009), and $\bar{\beta}$ is the slope of magnetostriction versus increment of temperature at the saturation magnetization, Jin et al. (2012). The derivation of the fourth part in Eq. (5) (i.e., the expressions involving $M_kM_lM_pM_q$) is analogous to the third part, and can be written as

$$\begin{aligned} & -\frac{1}{24}\left[\frac{\partial^5 G}{\partial\sigma_{ij}\partial M_k\partial M_l\partial M_p\partial M_q}-\frac{\partial^6 G}{\partial\sigma_{ij}\partial\sigma_{mn}\partial M_k\partial M_l\partial M_p\partial M_q}\sigma_{mn}\right. \\ & \left.-\frac{\partial^6 G}{\partial\sigma_{ij}\partial M_k\partial M_l\partial M_p\partial M_q\partial\theta}(\theta-\theta_0)\right]M_kM_lM_pM_q \\ & =-\frac{1}{M_{ws}^4}\left[\frac{3\lambda_s}{2}M_i^2M_j^2+\frac{2\bar{\beta}(\theta-\theta_0)-\lambda_s}{2}M_k^2M_k^2\delta_{ij}\right] \end{aligned} \tag{10}$$

Consequently, Eq. (5) for the strain components takes the final form

$$\begin{aligned} \epsilon_{ij} &= \frac{1}{E}\left[(1+\nu)\sigma_{ij}-\nu\sigma_{kk}\delta_{ij}\right]+\bar{\alpha}(\theta-\theta_0)\delta_{ij}+\frac{\lambda_s}{\sigma_s}\bar{\sigma}_{ij}+\frac{3\lambda_s}{2M_{ws}^2}M_iM_j \\ &- \frac{M_kM_k}{M_{ws}^2}\left[\frac{\lambda_s}{2}\delta_{ij}+\frac{\lambda_s}{\sigma_s}\bar{\sigma}_{ij}-\bar{\beta}(\theta-\theta_0)\delta_{ij}\right] \\ &- \frac{1}{M_{ws}^4}\left[\frac{3\lambda_s}{2}M_i^2M_j^2+\frac{2\bar{\beta}(\theta-\theta_0)-\lambda_s}{2}M_k^2M_k^2\delta_{ij}\right], \quad i,j=1,2,3 \end{aligned} \tag{11}$$

As to Eq. (6), it consists of six parts. The first and second part are independent of the stress and represent the nonlinear magnetization and thermal effects. Following Jin et al. (2012), these two parts can be written as:

$$\left[\frac{\partial^2 G}{\partial M_k\partial M_l}+\frac{\partial^3 G}{\partial M_k\partial M_l\partial\theta}(\theta-\theta_0)\right]M_l$$

$$+ \frac{1}{6}\left[\frac{\partial^4 G}{\partial M_k \partial M_l \partial M_p \partial M_q} + \ldots + \frac{\partial^5 G}{\partial M_k \partial M_l \partial M_p \partial M_q \partial \theta}(\theta - \theta_0)\right] M_l M_p M_q + \ldots$$
$$= \mu_0 \frac{1}{k^\theta M} L^{-1}\left(\frac{M}{M_s^\theta}\right) M_k \tag{12}$$

where $M = \sqrt{M_k M_k}$ and $L^{-1}(.)$ is the inverse of the Langevin function $L(x) = \coth(x) - 1/x$, which is based on the Boltzmann statistics and adopted by many works for ferromagnetic materials (e.g. Jiles and Atherton (1984), Smith (2005) and Zhou et al. (2009)). In addition, $k^\theta = 3\chi_m / M_s^\theta$ is a relaxation factor with χ_m being the susceptibility, and M_s^θ is the temperature-related saturation magnetization which can be expressed as

$$M_s^\theta = M_s \sqrt{\frac{\theta_c - \theta}{\theta_c - \theta_0}} \tag{13}$$

where θ_c is the Curie temperature and Kelvin temperature units should be employed.

The third and fourth parts in Eq. (6) are related to the inverse of the magnetostrictive effect yielding, which come from the magneto-elastic coupling terms of Eq. (4), and can be expressed as Zhou et al. (2009),

$$\left[\frac{\partial^3 G}{\partial \sigma_{ij} \partial M_k \partial M_l}\sigma_{ij} + \frac{1}{2}\frac{\partial^4 G}{\partial \sigma_{ij} \partial \sigma_{mn} \partial M_k \partial M_l}\sigma_{ij}\sigma_{mn}\right] M_l$$
$$+ \frac{1}{6}\left[\frac{\partial^5 G}{\partial \sigma_{ij} \partial M_k \partial M_l \partial M_p \partial M_q}\sigma_{ij} + \frac{1}{2}\frac{\partial^6 G}{\partial \sigma_{ij} \partial \sigma_{mn} \partial M_k \partial M_l \partial M_p \partial M_q}\sigma_{ij}\sigma_{mn}\right] M_l M_p M_q + \ldots$$
$$= -\frac{\lambda_s}{\mu_0 M_{ws}^2}\left[2\tilde{\sigma}_{kl} - \left(I_\sigma^2 - 3J_\sigma\right)\frac{\delta_{kl}}{\sigma_s}\right] M_l + \frac{\lambda_s}{\mu_0 M_{ws}^4}\left[\frac{3\lambda_s}{2}\delta_{ik}\delta_{jl} - \frac{\lambda_s}{2}\delta_{ij}\delta_{kl}\right]\sigma_{ij} M_l^3 \tag{14}$$

where $I_\sigma = \sigma_{kk}$ and $J_\sigma = \left(I_\sigma^2 - \sigma_{ij}\sigma_{ij}\right)/2$.

Finally, the fifth and sixth parts in Eq. (6) represent the magneto-thermo-elastic coupling effect, which come from the magneto-thermo-elastic coupling terms of Eq. (4), the same as those dependent on theta in Eq. (5):

$$\frac{\partial^4 G}{\partial \sigma_{ij} \partial M_k \partial M_l \partial \theta}\sigma_{ij} M_l(\theta - \theta_0) + \frac{1}{6}\frac{\partial^6 G}{\partial \sigma_{ij} \partial M_k \partial M_l \partial M_p \partial M_q \partial \theta}\sigma_{ij} M_l M_p M_q(\theta - \theta_0)$$
$$= -\frac{2\beta}{M_{ws}^2} I_\sigma M_l \delta_{kl}(\theta - \theta_0) + \frac{2\beta}{M_{ws}^4} I_\sigma M_l^3 \delta_{kl}(\theta - \theta_0) \tag{15}$$

The first term in this equation is similar to the magneto-thermo-elastic coupling term that was established by Jin et al. (2012), and the derivation of the second term is analogous to the first term.

The final form of Eq. (6) for the magnetic field components can be written as follows

$$\begin{aligned} H_k &= \frac{1}{k^\theta M^{an}} L^{-1}\left(\frac{M^{an}}{M_s^\theta}\right) M_k^{an} - \frac{\lambda_s}{\mu_0 M_{ws}^2}\left[2\tilde{\sigma}_{kl} - \left(I_\sigma^2 - 3J_\sigma\right)\frac{\delta_{kl}}{\sigma_s}\right] M_l^{an} \\ &+ \frac{\lambda_s}{\mu_0 M_{ws}^4}\left[\frac{3\lambda_s}{2}\delta_{ik}\delta_{jl} - \frac{\lambda_s}{2}\delta_{ij}\delta_{kl}\right]\sigma_{ij}(M_l^{an})^3 \\ &- \frac{2\tilde{\beta}(\theta-\theta_0)I_\sigma}{\mu_0}\left[\frac{M_k^{an}}{M_{ws}^2} - \frac{(M_k^{an})^3}{M_{ws}^4}\right], \qquad k = 1,2,3 \end{aligned} \tag{16}$$

It should be noted that due to the considered hysteretic effects in the following, Eq. (15) forms an expression for the anhysteretic magnetization Man which incorporates the effects of reversible magnetic domain motions, but does not account for irreversible domain wall bowing and translation. However, the consideration of domain wall energy yields additional reversible and irreversible components to the magnetization. The motion of domain walls when subjected to an applied magnetic field is impeded by the presence of the defects in the solid such as inhomogeneous internal stress or non-magnetic inclusions or voids. According to the assumption of Jiles and Atherton (1984), all of the nature of those imperfections could be taken as pinning sites, which therefore characterize the magnitude of hysteresis property of ferromagnetic materials. The pinning energy of a site is proportional to μ0He · (m−m ′), where m and m ′ are the magnetic moment per unit volume of a magnetic domain and its adjacent one, respectively, and He is the effective field which can be expressed as

$$\begin{aligned} H_k^e &= H_k + \frac{\lambda_s}{\mu_0 M_{ws}^2}\left[2\tilde{\sigma}_{ij} - (I_\sigma^2 - 3J_\sigma)\frac{\delta_{kl}}{\sigma_s}\right] M_l^{an} - \frac{\lambda_s}{\mu_0 M_{ws}^4}\left[6\sigma_{kl} - 2\sigma_{ii}\delta_{kl}\right](M_l^{an})^3 \\ &+ \frac{2\tilde{\beta}(\theta-\theta_0)I_\sigma}{\mu_0}\left[\frac{M_k^{an}}{M_{ws}^2} - \frac{(M_k^{an})^3}{M_{ws}^4}\right] \end{aligned} \tag{17}$$

It can be shown that the magnetic-energy balance equation is given by

$$\int \mu_0 M_i^{irr} dH_i^e = \int \mu_0 M_i^{an} dH_i^e - \mu_0 K_j \zeta \int \frac{dM_j^{irr}}{dH_i^e} dH_i^e \tag{18}$$

where K_j are pining constants and the parameter ζ takes the value $+1$ when the magnetic field increases and -1 when it decreases which ensures that the pinning opposes changes in magnetization. Differentiating this relation with respect to H_i^e yields

$$M_i^{irr} = M_i^{an} - K_j \zeta \frac{dM_j^{irr}}{dH_i^e} \tag{19}$$

Differentiating Eq. (17) yields

$$dH_i^e = dH_i + \xi_{ij}^{(1)} dM_j^{an} + \xi_{ij}^{(2)} d(M_j^{an})^3 \equiv dH_i + A_{ij} dM_j^{an} \tag{20}$$

The reversible magnetization can be expressed as

$$M_i^{rev} = c\left(M_i^{an} - M_i^{irr}\right) \tag{21}$$

where c is the ratio of the initial magnetic susceptibility to the initial anhysteretic susceptibility.
In this equation, M_i^{an} are determined from Eq. (16) and M_i^{irr} can be computed by integrating Eq. (19).
The total hysteretic magnetization is given as

$$M_i = M_i^{rev} + M_i^{irr} \tag{22}$$

Hence the total magnetization Mi can be nonlinearly expressed in terms of magnetic fieldH_i, stresses σ_{ij} and temperature θ. Consequently, relations (11) and (22) form the final nonlinear anisothermal constitutive equations which govern the response of magnetostrictive material that exhibits hysteretic effects during loading and unloading.

The governing equations consist of the equilibrium equations which in the absence of body forces are given by

$$\sigma_{ij,j} = 0 \tag{23}$$

For the magnetic field, the Maxwell equation

$$B_{i,i} = 0 \tag{24}$$

where B_i are the components of the magnetic flux density vector, should be satisfied. The components of B_i are related to the magnetic field intensity components H_i and magnetization components M_i in the form

$$B_i = \mu_0 (H_i + M_i) \tag{25}$$

In the present steady state case and absence of conduction current, $\nabla \times \boldsymbol{H} = \boldsymbol{0}$ so that $\boldsymbol{H} = -\nabla\psi$ where ψ is the magnetic potential. Consequently, the magnetostrictive constitutive equations

can be presented by σ_{ij} and B_i, expressed in terms of ϙij and H_i or equivalently, in terms of the mechanical displacement components ui and the magnetic potential ψ.

At the interface between two materials the following jump conditions must be imposed.

$$[\sigma_{ij}]N_j = 0, \quad [u_i] = 0, \quad [B_i]N_i = 0, \quad [\psi] = 0 \tag{26}$$

where N_i are the components of the normal vector to the interface between the materials.

The magnetostrictive constitutive equations (1)-(22) and (25) are nonlinear. As discussed by Aboudi et al. (2014), the nonlinearity of these equations necessitates the formulation of these equations in an incremental form. The use of this formulation in the micromechanics analysis provides at each increment of loading a system of linear algebraic equations which is obviously a great advantage over nonlinear ones. To this end, let the two vectors $\Delta \boldsymbol{X}$ and $\Delta \boldsymbol{Y}$ be defined as follows

$$\begin{aligned} \Delta \boldsymbol{X} &= [\Delta\epsilon_{11}, \Delta\epsilon_{22}, \Delta\epsilon_{33}, 2\Delta\epsilon_{23}, 2\Delta\epsilon_{13}, 2\Delta\epsilon_{12}, -\Delta H_1, -\Delta H_2, -\Delta H_3] \\ \Delta \boldsymbol{Y} &= [\Delta\sigma_{11}, \Delta\sigma_{22}, \Delta\sigma_{33}, \Delta\sigma_{23}, \Delta\sigma_{13}, \Delta\sigma_{12}, \Delta B_1, \Delta B_2, \Delta B_3] \end{aligned} \tag{27}$$

By following and generalizing the incremental procedure that has been presented in Aboudi et al. (2014), the final form of the soft ferromagnetic constitutive relations (1)-(22) and (25) cast in an incremental form, can be expressed by the following compact relation:

$$\Delta \boldsymbol{Y} = \boldsymbol{Z}\Delta \boldsymbol{X} - \boldsymbol{\Gamma}\Delta\theta \tag{28}$$

where Z is the instantaneous magneto-elastic symmetric matrix of the 9th-order and ¡ is the instantaneous thermal vector of nine components. These equations represent the instantaneous behavior of the soft ferromagnetic phases of the composite.

III. MICROMECHANICS ANALYSIS OF SOFT FERROMAGNETIC COM- POSITES

The details of the HFGMC micromechanics analysis of magnetostrictive composites have been presented by Aboudi et al. (2014). It is not necessary to derive the details of the generalization to soft ferromagnetic composites. Therefore this analysis is briefly described in the following.

Consider a particulate periodic composite in which some of the phases are soft ferromagnetic materials. The composite is described with respect to the global coordinates (x1, x2, x3), see Fig. 1(a). Figure 1(b) shows a repeating unit cell (RUC), defined with respect to local coordinates (y1, y2, y3), of the periodic composite. The parallelepiped RUC of the composite is divided in to

N_α, N_β and N_γ subcells in the y_1, y_2 and y_3 directions, respectively. Each subcell is labeled by the indices $(\alpha\beta\gamma)$ with $\alpha = 1, ..., N_\alpha$, $\beta = 1, ..., N_\beta$ and $\gamma = 1, ..., N_\gamma$. The dimensions of subcell $(\alpha\beta\gamma)$ in the y_1, y_2 and y_3 directions are denoted by d_α, h_β and l_γ, respectively. A local coordinate system $(\bar{y}_1^{(\alpha)}, \bar{y}_2^{(\beta)}, \bar{y}_3^{(\gamma)})$ is introduced in each subcell whose origin is located at its center, see Fig. 1(c).

Figure 1 shows the case in which the repeating unit cell consists of a spherical soft ferromag- netic inclusion embedded within a matrix thus forming a two-phase composite. The inclusion can be chosen to fill just one subcell which is sufficient for the prediction of the macroscopic (global) behavior of the composite. If however the detailed distribution of the field within the repeating unit cell is sought, it is necessary to discretize the spherical inclusion into several subcells all of which approximate the spherical shape for a given volume fraction. This is well illustrated by

Fig. 1(b). For example, in order to establish the field distribution in the magnetostrictive par- ticulate composite discussed in Aboudi et al. (2014), the repeating unit cell has been discretized into 40×40×40 subcells in the three orthogonal directions with the spherical inclusion occupying 1/4 of its volume.

In the framework of HFGMC, the increments of the mechanical displacement vector $\Delta \boldsymbol{u}^{(\alpha\beta\gamma)}$ and magnetic potential $\Delta\psi^{(\alpha\beta\gamma)}$ in the subcell $(\alpha\beta\gamma)$ are expanded into second-order polynomials. To this end, let the vector $\Delta \boldsymbol{W}^{(\alpha\beta\gamma)}$ in the subcell includes the displacement increments $\Delta \boldsymbol{u}^{(\alpha\beta\gamma)}$ and the magnetic potential increment $\Delta\psi^{(\alpha\beta\gamma)}$:

$$\Delta \boldsymbol{W}^{(\alpha\beta\gamma)} = \left[\Delta u_1, \Delta u_2, \Delta u_3, \Delta\psi\right]^{(\alpha\beta\gamma)} \tag{29}$$

The 2nd-order expansion of $\Delta \boldsymbol{W}^{(\alpha\beta\gamma)}$ is given by

$$\begin{aligned}\Delta \boldsymbol{W}^{(\alpha\beta\gamma)} &= \Delta \boldsymbol{W} + \Delta \boldsymbol{W}^{(\alpha\beta\gamma)}_{(000)} + \bar{y}_1^{(\alpha)} \Delta \boldsymbol{W}^{(\alpha\beta\gamma)}_{(100)} + \bar{y}_2^{(\beta)} \Delta \boldsymbol{W}^{(\alpha\beta\gamma)}_{(010)} + \bar{y}_3^{(\gamma)} \Delta \boldsymbol{W}^{(\alpha\beta\gamma)}_{(001)} \\ &+ \frac{1}{2}\left(3\bar{y}_1^{(\alpha)2} - \frac{d_\alpha^2}{4}\right) \Delta \boldsymbol{W}^{(\alpha\beta\gamma)}_{(200)} + \frac{1}{2}\left(3\bar{y}_2^{(\beta)2} - \frac{h_\beta^2}{4}\right) \Delta \boldsymbol{W}^{(\alpha\beta\gamma)}_{(020)} + \frac{1}{2}\left(3\bar{y}_3^{(\gamma)2} - \frac{l_\gamma^2}{4}\right) \Delta \boldsymbol{W}^{(\alpha\beta\gamma)}_{(002)}\end{aligned} \tag{30}$$

where $\Delta \bar{\boldsymbol{W}} = \left[\Delta\bar{\boldsymbol{\epsilon}} \cdot \boldsymbol{x}, -\Delta \bar{\boldsymbol{H}} \cdot \boldsymbol{x}\right]$ consists of the externally applied magneto-mechanical loading, and the coefficients $\Delta \boldsymbol{W}^{(\alpha\beta\gamma)}_{(lmn)}$ are determined by implementing the equilibrium (23) and Maxwell (24) equations, together with the interfacial conditions given by Eq. (26). In addition, periodic conditions must be imposed to ensure that the tractions, mechanical displacements, normal magnetic flux density and magnetic potential are equal at the opposite sides of the repeating unit cell. At each increment of loading, the presently generalized micromechanical analysis results into a system of $24N_\alpha N_\beta N_\gamma$ algebraic equations. The solution of these equations provides the current values of the magneto-mechanical and thermal concentration tensors.

Let $\Delta \bar{\boldsymbol{X}}$ denote the externally applied far-field magneto-mechanical loading:

$$\Delta \bar{\boldsymbol{X}} = \left[\Delta\bar{\epsilon}_{11}, \Delta\bar{\epsilon}_{22}, \Delta\bar{\epsilon}_{33}, 2\Delta\bar{\epsilon}_{23}, 2\Delta\bar{\epsilon}_{13}, 2\Delta\bar{\epsilon}_{12}, -\Delta\bar{H}_1, -\Delta\bar{H}_2, -\Delta\bar{H}_3\right] \tag{31}$$

and $\Delta \boldsymbol{Y}$ represents the average of all $\Delta \boldsymbol{Y}^{(\alpha\beta\gamma)}$ (i.e., averaged over all subcells $(\alpha\beta\gamma)$ of the composite). By following the HFGMC micromechanics analysis that has been presented by Aboudi et al. (2014), concentration tensors $\boldsymbol{A}^{(\alpha\beta\gamma)}$, $\boldsymbol{A}^{th(\alpha\beta\gamma)}$ can be established such that the local magnetoelastic field in subcell $(\alpha\beta\gamma)$ can be related to the externally applied loading $\Delta \bar{\boldsymbol{X}}$ and temperature increment $\Delta\theta$ in the form

$$\Delta \boldsymbol{X}^{(\alpha\beta\gamma)} = \boldsymbol{A}^{(\alpha\beta\gamma)} \Delta \bar{\boldsymbol{X}} + \boldsymbol{A}^{th(\alpha\beta\gamma)} \Delta\theta \tag{32}$$

Consequently, the following macroscopic (global) incremental constitutive equation of the soft ferromagnetic composite can be established

$$\Delta \bar{\boldsymbol{Y}} = \boldsymbol{Z}^* \Delta \bar{\boldsymbol{X}} - \boldsymbol{\Gamma}^* \Delta\theta \tag{33}$$

In this relation, $\mathbf{Z}^*$ is the effective instantaneous tangent 9×9 matrix of the soft ferromagnetic composite, and $\mathbf{\Gamma}^*$ is the instantaneous effective thermal stress-magnetic 9-th order vector, both of which are determined from the current values of the established concentration tensors. It should be noted that the micromechanical analysis determines the elements of $\mathbf{Z}^*$ and $\mathbf{\Gamma}^*$ in terms of the material properties, geometrical sizes of the subcells and current values of the magneto-elastic field, in an explicit (albeit complicated) manner.

Applications are given for a particulate soft ferromagnetic material/epoxy composite. The material properties of the soft ferromagnetic material are given in Table 1. These material parameters have been determined by fitting the behavior of the soft ferromagnetic constituent with the experimental data of Gorkunov et al. (2013). The epoxy matrix material constants are given in Table 2.

IV. APPLICATIONS

The micromechanical theory, in which the incremental form of the generalized constitutive equa- tions of the soft ferromagnetic material have been included as a phase, is presently applied to investigate the response of soft ferromagnetic composites under various circumstances. The material properties of a medium carbon steel rod are given in Table 1. These material parameters have been determined by fitting the behavior of the soft ferromagnetic constituent with the experimental data of Gorkunov et al. (2013). A comparison between the axial strain ϱ11 vs. magnetic field H1 prediction of the established constitutive equations for ferromagnetic materials and the experimental data of Gorkunov et al. (2013) is shown in Fig. 2(a). It can be readily obsereved
that the proposed constitutive relations are capable of predicting the magnetostrictive strain of the soft ferromagnetic material at different stress and magnetic field levels. Applications are given in the following for a particulate soft ferromagnetic material/epoxy composite.
The epoxy matrix material constants are given in Table 2.

4.1 The Behavior Of The Soft Ferromagnetic Material

In Fig. 2(b), the response of the soft ferromagnetic material at room temperature that is subjected to a complete cycle of loading-unloading by a magnetic field applied in the 1-direction is shown. This figure exhibits the induced axial ϵ_{11} and transverse $\epsilon_{22} = \epsilon_{33}$ magnetostrictive strains, magnetic flux density B_1 and the magnetization M_1. It should be noted that with the present material constants, the hysteresis loop is quite narrow.

The response of the soft ferromagnetic material at room temperature that is subjected to an axial tensile and compressive pre-stresses: $\sigma_{11}^0 = 50$ and -50 MPa, is shown in Fig. 3. Also included for comparison is the behavior in the absence of a pre-stress. Figure 3(a)-(b) exhibit the axial and transverse magnetostrictions, and Figure 3(c) depicts the magnetic flux densities. In Figure 3(d), the resulting nonlinear characteristics of relative permeabilities μ/μ_0 are also compared among these three cases.

As a final illustration of the behavior of the soft ferromagnetic material, comparisons between the responses of the material at elevated temperatures: $\theta - \theta_0 = 25$K, 50K, and at room temperature, $\theta = \theta_0$, are shown in Fig. 4. It should be noted that the temperature has an appreciable

As a first step in investigating the behavior of the soft ferromagnetic composite, the effect of changing the volume fraction v_f of the ferromagnetic material on the composite response is considered. In the absence of an applied pre-stress, the global (overall) behavior of the composite at room temperature that is subjected to a magnetic field in the axial 1-direction is shown in Fig. 5 for -v_f = 0.5, 0.7, 0.95 and 1.0 (v_f = 1 implies a monolithic soft ferromagnetic material). It is clearly observed that the macroscopic magnetostrictions $\overline{\varepsilon}_{11}$ and $\overline{\varepsilon}_{22}$ in the axial and transverse directions, as well as the global magnetic flux density $\overline{B}_1$ and the effective relative permeability μ^*/μ_0 are strongly dependent on the ferromagnetic inclusion volume fraction.

When the composite is subjected to a pre-stress σ_{11}^0 = 50MPa that is applied in the 1- direction, the resulting macroscopic response is shown in Fig. 6 for four values of v_f. A comparison of this figure with Fig. 5 reveals the effect of the applied pre-stress. Figure 7 on the other hand displays the effect of applying pre-temperature deviation of $\theta - \theta_0$ =50 K on the composite. The comparisons of both Fig. 6 and Fig. 7 with Fig. 5 show that the magnetostrictions are the most affected values by the application of pre-stress and pre-temperature on the composite. This is more clearly shown in Fig. 8 where the effect of applied pre-temperatures on the composite with v_f =0.95 is exhibited.

As a final illustration, Fig. 9 shows the soft ferromagnetic composite response when the magnetic field is applied in both 1 and 2-directions. In this figure, the response of the composite with v_f = 0.95 is compared with that of the monolithic ferromagnetic material (v_f = 1) exhibiting the effect of the biaxial magnetic loading on the magnetostrictions, magnetic flux densities and the relative permeability.

V. CONCLUSIONS

Multiaxial nonlinear isothermal constitutive equations that have been presented by Zhou et al. (2009) for the modeling of soft ferromagnetic materials have been presently generalized to include magneto-thermo-elastic coupled effects in conjunction with hysteretic behavior. The calibrated constitutive relations of the soft ferromagnetic material have been shown to be capable of predicting the magnetostrictive strain at different stress and magnetic field levels. Next, these constitutive equations are incorporated with the HFGMC micromechanical analysis for the prediction of the macroscopic (global) response of soft ferromagnetic particulate composites. The proposed modeling enables the prediction of the response of soft ferromagnetic composites subjected to pre-stresses, pre-temperature followed by the application of a combined magneto-thermo-elastic loading.

As shown, the present micromechanical theory is capable of predicting the effective perme- ability of the composite an its variation with the applied loading. Permeability is a measure of the ability to magnetize the material, and in using soft ferromagnetic composites, it is desirable to obtain the highest value of effective

permeability. The present micromechanical can be easily employed by the designer to predict this property by selecting possible desired properties of the phases. The present micromechanical modeling can be further extended to include the effect of ex-isting porosities in the composites. If desired, the shape of the ferromagnetic particles and their microstructural distribution can be also included in the offered model.

ACKNOWLEDGMENT

The first and second authors gratefully acknowledge the supports by the Fund of National Natural Science Foundation of China (Nos.11672217,11402105).

Table 1. Material properties of the soft ferromagnetic material.

Property	Value
E	210 GPa
ν	0.25
$\bar{\alpha}$	12×10^{-6} K^{-1}
β	-1.3×10^{-7} K^{-1}
θ_0	293 K
θ_c	656.3 K
λ_s	16×10^{-6}
M_s	1000 kA/m
M_{ws}	730 kA/m
σ_s	400 MPa
χ_m	35
K	3.283 kA/m
c	0.1

Table 2. The parameters of the thermoelastic epoxy matrix.

E (GPa)	ν	$\bar{\alpha}(10^{-6}$ K$^{-1})$
3	0.35	54

References

[1]. J. Aboudi, S.M. Arnold, B.A. Bednarcyk, Micromechanics of Composite Materials: A General- ized Multiscale Analysis Approach, Elsevier, Oxford, UK, 2013.
[2]. J. Aboudi, X. Zheng, K. Jin, Micromechanics of magnetostrictive composites, Int. J. Eng. Sci. 81 (2014), 82-99.
[3]. S. Bednarek, Magnetoelastic properties of a ferrelast within an organo-silicon polymer matrix, J. Magnet. Mag. Mater. 166 (1997), 91-96.
[4]. E. Bayramli, O. Golgelioglu, H.B. Ertan, Power metal development for electrical motor applica- tions, J. Mater. Process. Tech. 161 (2005), 83-88.
[5]. M.M. Dias, H.J. Mozetic, J.S. Barboza, R.M. Martins, L. Pelegrini, L. Schaeffer, Influence of resin type and content on electrical and magnetic properties of soft magnetic composites, Powder Tech. 237 (2013), 213-220.
[6]. E.S. Gorkunov, Yu. V. Subachev, A.M. Povolotskaya, S.M. Sadvorkin, The influence of an elastic uniaxial deformation of a medium-carbon steel on its magnetostriction in the longitudinal and transverse directions, Russian J. Nondestruct. Testing 49 (2013), 584-594.
[7]. P. Gramatyka, R. Nowosielski, P. Sakiewicz, T. Raszka, Soft magnetic composites based on nanocrystalline Fe73.5Cu1Nb3Si13.5B9 and Fe powders, J. Achiev. Mater. Manufac. Eng. 15 (2006), 27-31.

[8]. Y.G. Guo, J.G. Zhu, J.J. Zhong, Core losses un claw pole permament magnet machines with soft magnetic composite stators, IEEE Trans. on Magnetics 39 (2003), 3199-3201.
[9]. Hamler, V. Gorican, B. Sustarsic, A. Sirc, The use of soft magnetic composite materials in synchronous electric motor, J. Magnet. Mag. Mater. 304 (2006), e816-e819.
[10]. L.O. Hultman, A.G. Jack, Soft magnetic composites-materials and applications, IEEE conference vol. 1 (2003), 516-622. DOI: 1109/IEMDC.2003.1211312. 18
[11]. D.C. Jiles, Theory of the magnetomechanical effect, J. Physics D: Appl. Phys. 28 (19995, 1537- 1546.
[12]. D.C. Jiles, D.L. Atherton, Theory of ferromagnetic hysteresis, J. Appl. Phys. 55 (1984), 2115- 2120.
[13]. K. Jin, Y. Kou, X. Zheng, A nonlinear magneto-thermo-elastic coupled hysteretic constitutive model for magnetostrictive alloys, J. Magnet. Mag. Mater. 324 (2012), 1954-1961.
[14]. M.B. Moffet, A.E. Clark, M. Wun-Fogle, J. Linberg, J.P. Teter, E.A. McLaughlin, Characteriza- tion of Terfenol-D for magnetostrictive tranducers. J. Acoust. Soc. Am. 89 (1991), 1448-1455.
[15]. R. Nowosielski, Soft magnetic polymer-metal composites consisting of nanostrutural Fe-basic poders. J. Achiev. Mater. Manufac. Eng. 24 (2007), 68-77.
[16]. J.H. Paterson, R. Devine, A.D.R. Phelps, Complex permeability of soft magnetic ferrite/polyester resin composites at frequencies above 1 MHz, J. Magnet. Mag. Mater. 196-197 (1999), 394-396.
[17]. R. Ruffini, N. Vyshinskaya, V. Nemkov, R. Goldstein, C.J. Yakey, Innovations in soft magnetic composites and their applications in induction systems, Fluxtrol Inc., Auburn Hills, MI, USA. M. Streckova, L. Medvecky, J. Fuzer, P. Kollar, R. Bures, M. Faberova, Design of novel soft magnetic composites based on Fe/resin modified with silica, Mater. Lett. 101 (2013), 37-40.
[18]. M. Streckova, R. Bures, M. Faberova, L. Medvecky, J. Fuzer, P. Kollar, A comparison of soft mag- netic composites designed from different ferromagnetic powders and phenolic resins, Chinese J. Chem. Eng. 23 (2015), 736-743.
[19]. L. Svensson, K. Frogner, P. Jeppsson, T. Cedell, A. Andersson, Soft magnetic moldable compos- ites: properties and applications, J. Magnet. Mag. Mater. 324 (2012), 2717-2722.
[20]. H. Shokrollahi, K. Janghorban, Soft magnetic composite materials (SMCs), J. Materl. Pro- cess.Tech. 189 (2007), 1-12. R. C. Smith, Smart Material Systems: Model Development, siam, Philadelphia, 2005.
[21]. M. Tada and K. Suzuki, US Patent US6338900 B1, 2002. 19
[22]. H-M. Zhou, Y-H. Zhou, X-J. Zheng, Q. Ye, J. Wei, A general 3-D nonlinear magnetostrictive constitutive model for soft ferromagnetic materials, J. Magn. Magn. Mater. 321, (2009), 281- 290.

Figure Captions

Fig. 1: (a) A triply-periodic particulate composite, defined with respect to global coordinates (x_1, x_2, x_3). (b) A repeating unit cell (RUC), represented with respect to local coordinates (y_1, y_2, y_3). Its dimensions in the y_1, y_2 and y_3 directions are D, H and L, respectively. It is divided into N_α, N_β and N_γ subcells, in the y_1, y_2 and y_3 directions, respectively. (c) A characteristic subcell $(\alpha\beta\gamma)$ with local coordinates $\bar{y}_1^{(\alpha)}, \bar{y}_2^{(\beta)}$ and $\bar{y}_3^{(\gamma)}$ whose origin is located at its center.

Fig. 2: (a) Axial strain ϵ_{11} against magnetic field H_1. Comparsions between the experimental data, Gorkunov et al. (2013), and model predictions for magnetostrictive strain of steel under different compressive stress (points: experimental data; lines: model predictions). (b) The response of the soft ferromagnetic material subjected to a cyclic magnetic field H_1 applied in the 1-direction showing the induced axial strain ϵ_{11}, transverse strai ϵ_{22}, axial magnetic flux density B_1 and axial magnetization M_1.

Fig. 3: The response of the soft ferromagnetic material subjected to an applied magnetic field H_1 in the 1-direction. The material has been initially subjected to three values of pre-stresses: $\sigma_{11}^0 = 50, 0$ and -50 MPa. (a) Induced axial strain, (b) transverse strain, (c) axial magnetic flux density and, (d) relative permeability.

Fig. 4: The response of the soft ferromagnetic material subjected to an applied magnetic field H_1 in the 1-direction. The material has been initially subjected to three values of temperatures: $\theta - \theta_0 = 50$K, 25K and 0K. (a) Induced axial strain, (b) transverse strain, (c) axial magnetic flux density and, (d) relative permeability.

Fig. 5: Comparisons between the behaviors of the soft ferromagnetic composite at room temperature subjected to a magnetic field $\bar{H}_1$ applied in the axial 1-direction for three values of particle volume ratios: $v_f = 0.5$, $v_f = 0.7$ and 0.95. Also shown is the response of the monolithic ferromagnetic material ($v_f = 1$). (a) Induced global axial strain, (b) global transverse strain, (c) global axial magnetic flux density and, (d) effective relative permeability.

Fig. 6: The soft ferromagnetic composite is at room temperature and subjected to a pre-stress σ_{11}^0=50 MPa applied in the axial direction. The composite is subsequently subjected to a magnetic field $\bar{H}_1$ in the axial 1-direction. Comparisons between the composite behavior for particle volume ratios: $v_f = 0.5$, $v_f = 0.7$ 0.95 and 1 are shown. (a) Induced global axial strain, (b) global transverse strain, (c) global axial magnetic flux density and, (d) effective relative permeability.

Fig. 7: The soft ferromagnetic composite is at elevated temperature $\theta - \theta_0 = 50$K. The composite is subsequently subjected to a magnetic field $\bar{H}_1$ applied in the axial 1-direction. Comparisons between the composite behavior for particle volume ratios: $v_f = 0.5$, $v_f = 0.7$ 0.95 and 1 are shown. (a) Induced global axial strain, (b) global transverse strain, (c) global axial magnetic flux density and, (d) effective relative permeability.

Fig. 8: Comparisons between the responses of the soft ferromagnetic composite with inclusion volume fraction $v_f = 0.95$ at room temperature and elevated temperatures: $\theta - \theta_0 = 0K, 25K and 50$K. The composite is subjected to a magnetic field $\bar{H}_1$ applied in the axial 1-direction. (a) Induced global axial strain, (b) global transverse strain, (c) global axial magnetic flux density and, (d) effective relative permeability.

Fig. 9: Comparisons between the behaviors of the soft ferromagnetic composite at room temperature subjected to a magnetic field $\bar{H}_1 = \bar{H}_2$ applied in the 1 and 2-directions, for an inclusion volume fractions $v_f = 0.95$ and the monolithic ferromagnetic material $v_f = 1$. (a) Induced global axial strain, (b) global transverse strain, (c) global axial magnetic flux density and, (d) effective relative permeability.

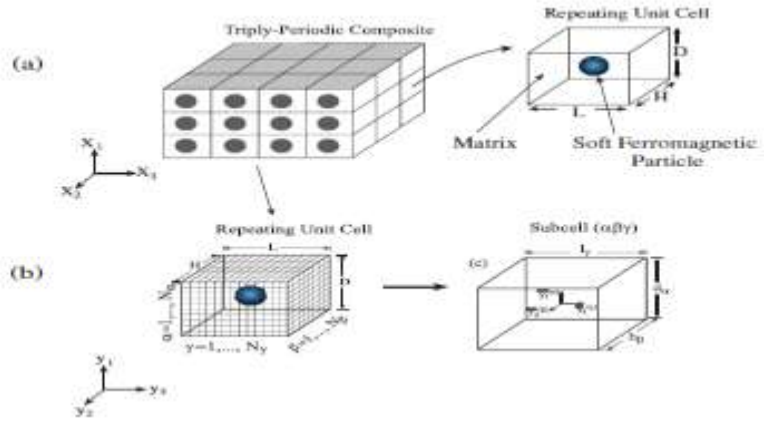

Fig.1

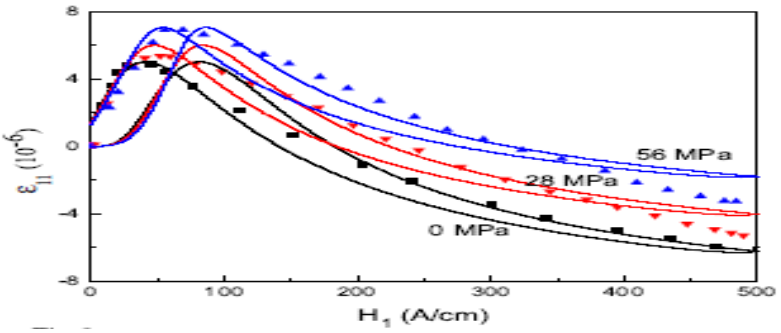

Fig-2

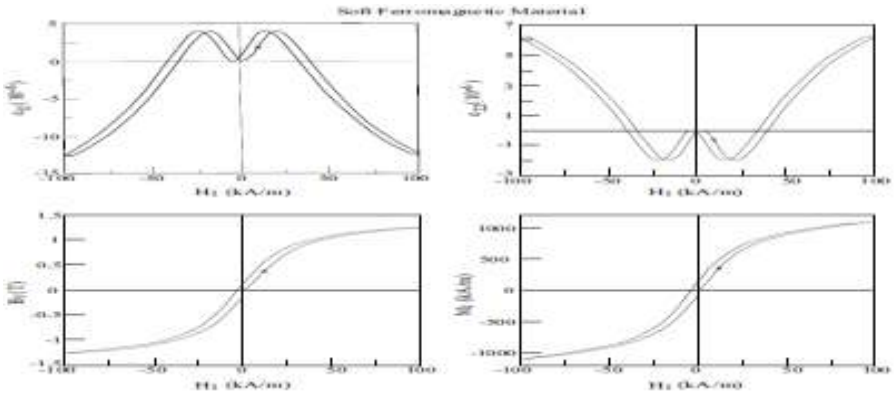

Fig-2b

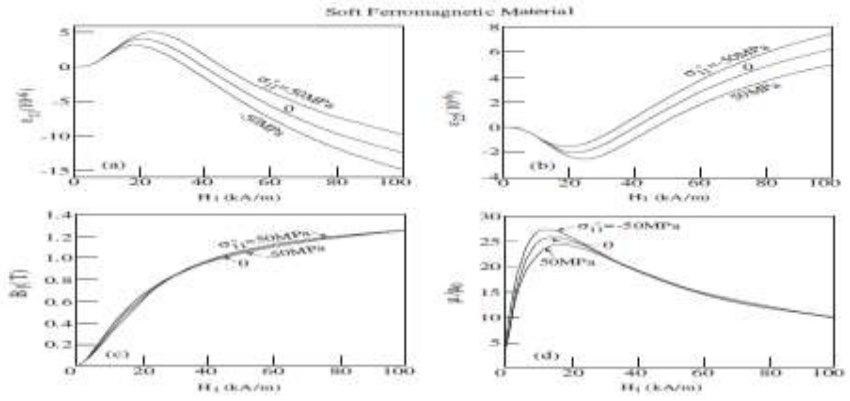

Fig-3

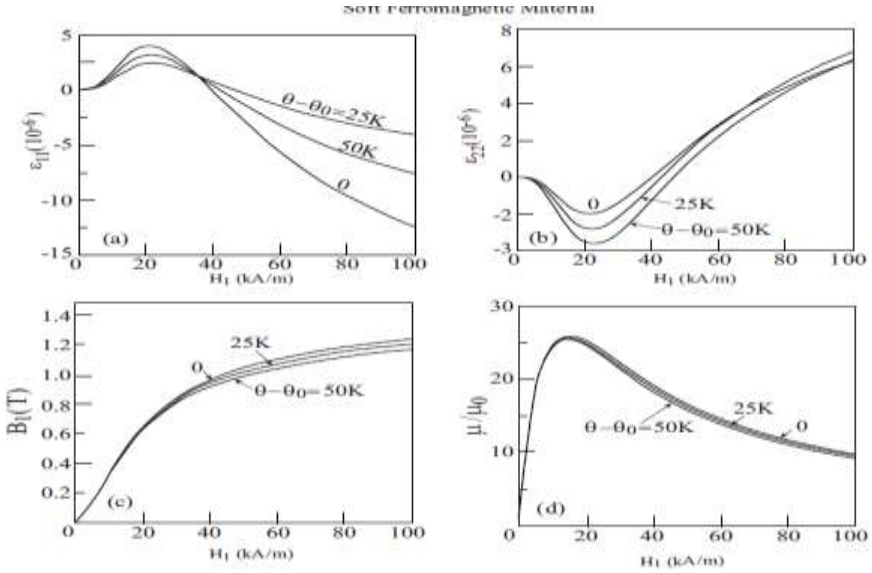

Fig-4

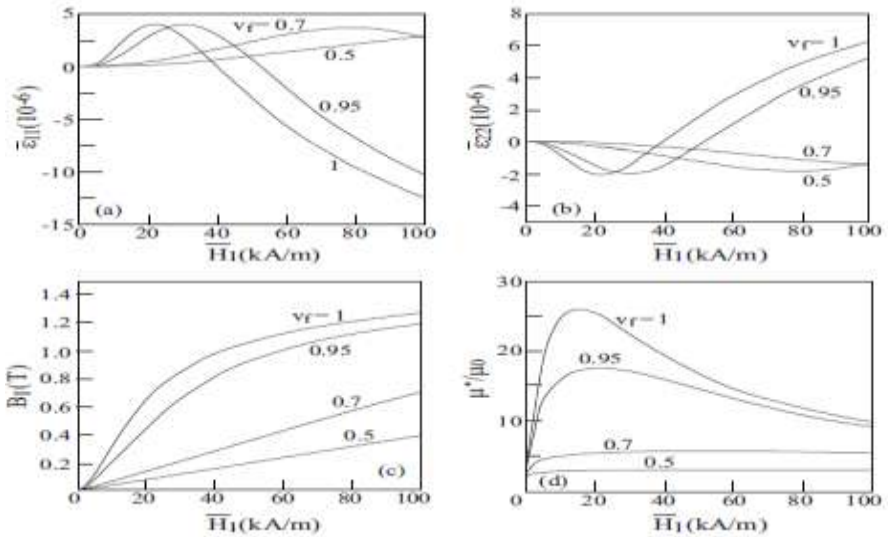

Fig-5

$\sigma_{11}^{\circ} = 50\,MPa$

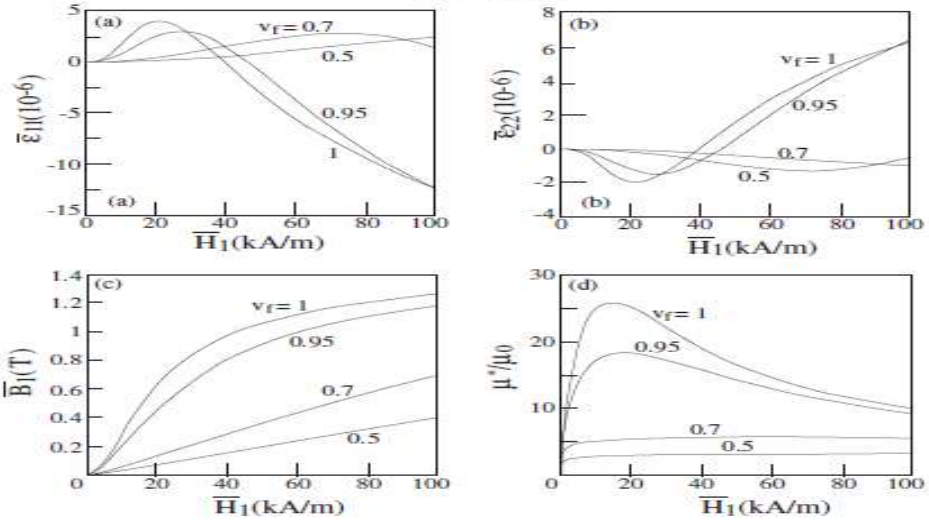

Fig-6

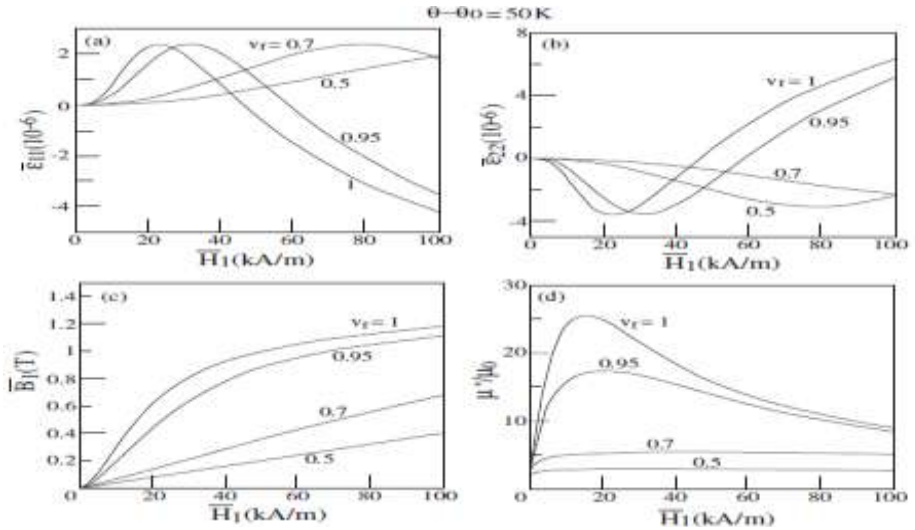

Fig-7

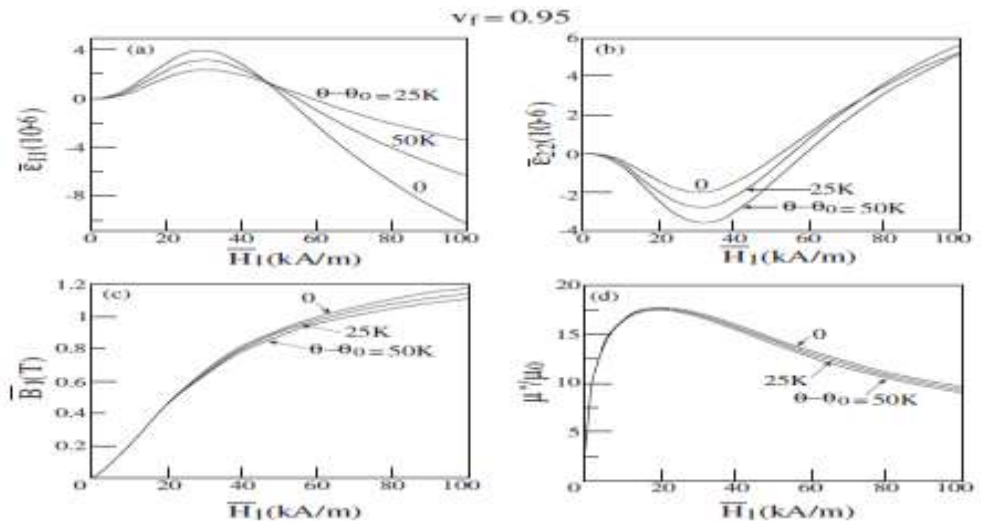

Fig-8

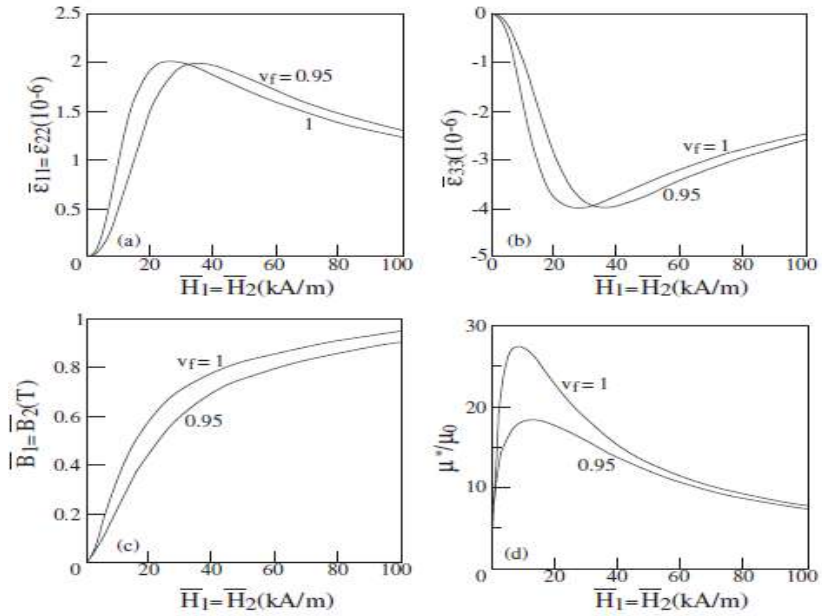

Fig-9